TOWARDS HIGH-QUALITY SELECTIVE BEAM MELTING TECHNOLOGIES: MODELING AND EXPERIMENTS OF SINGLE TRACK FORMATIONS

Wentao Yan*†, Wenjun Ge†, Jacob Smith*, Gregory Wagner*, Feng Lin†, and Wing Kam Liu*

*Department of Mechanical Engineering, Northwestern University, Evanston, IL 60201, U.S.
† Department of Mechanical Engineering, Tsinghua University, Beijing 100084, China

REVIEWED

Abstract

Additive manufacturing technologies are promising but still not widely used. One major problem is the unsatisfying quality e.g. surface roughness and dimensional accuracy. The discontinuous droplets and distortions in single track formations, which influence both surface roughness and dimensional accuracy, were investigated. The physical mechanisms of the formations of the droplets and distortions were proposed and the heat transfer simulations based on the Finite Element Method were established to predict the possibility of the droplet formation and the magnitude of the distortion. Experiments using Electron Beam Melting were then conducted to validate the physical and numerical models. The good agreements of the simulated and experimental results demonstrated that the proposed models are simple and efficient to provide quantitative predictions of the distortions.

Introduction

Additive manufacturing technologies are very promising. But they are still not widely industrialized as conventional manufacturing technologies e.g. casting and welding. One of the major problems to be solved is the unsatisfactory fabrication quality such as dimensional accuracy and surface roughness. Single track formations are the simplest but most efficient approach to investigate the problem of fabrication quality. The single track is the basic element of any components in any complex shapes, and the fabrication quality of the single track can determine the quality and the performance of the final product. Therefore, we conducted both modeling and experiments to specifically investigate the formations of discontinuous droplets and distorted single tracks in Selective Beam Melting (SBM). With thorough understanding of the formation mechanisms of the droplets and the distortions in single track formations, we can predict and even control the fabrication quality of the final products. The experimental images of droplets and a distorted single track are shown in Fig.1.

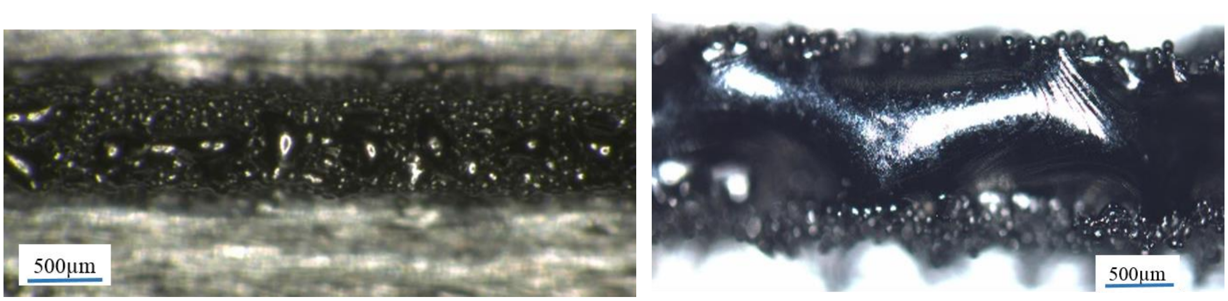

(a) discontinuous droplets (b) a distorted single track

Fig.1 Experimental images of discontinuous droplets and a distorted single track

Several researchers conducted investigations on the problems about droplets and distortions in Selective Laser Melting (SLM) and Electron Beam Melting (EBM), the two most typical SBM technologies. T. Childs et al.[1] treated the molten metal as an ideal cylinder of homogeneous liquid and attributed the Plateau-Rayleigh capillary instability of the molten liquid cylinder to the formation of the droplets in SLM. Yadroitsev et al. [2] modelled the molten metal as a segmental cylinder of homogeneous liquid, which is closer to the reality of AM. Based on the Plateau-Rayleigh capillary instability, they thought that the geometrical configuration with the smallest surface area was the most stable state. Then a criterion of the stability was derived from the geometrical analysis of the segmental cylinder shape. The capillary instability remains one of the most popular explanations for both the droplets and the distortions, which are often called "balling effect" [3]. Dai, D. and Gu, D. [4] employed the Volume of Fluid method (VOF) to model the flow of the molten pool in SLM to explain the formation mechanism of surface roughness of the top surface of the final product. Their model illustrated that the thermo-capillary force induced by the temperature gradient and the recoil pressure caused by the evaporation were dominant in the molten pool flow and the formation of surface roughness. All the aforementioned models and explanations treated the powder bed as an effective homogeneous continuum material. Korner et al. [5] employed Lattice Boltzmann Method (LBM) to establish a mesoscopic model to get the insight of the evolution process of the individual powders in EBM. The model revealed that the formation of droplets was due to the random arrangement of the powder bed and the effect of the capillary forces and wetting.

In this work, we propose physical models to explain the formation mechanisms of the droplets and the distortions, and then build a simple but efficient numerical heat transfer model to predict whether the droplets or the distorted tracks can be formed.. Experiments of single track formation were conducted using EBM to validate the physical and numerical models. The good agreement between experimental and simulated results demonstrated the reasonableness and feasibility of the proposed models. In some sense, the distortions of the single track in SBM could not be avoided due to the unavoidable random attachment between the melted metal and unmelted powders near the melting boundaries.

Physical and numerical model

The formation processes of discontinuous droplets and continuous single tracks are schematically shown in Fig.2. Given the same powder bed, the formation of droplets or continuous single track depends on the energy input. The energy input is determined mostly by the ratio between the beam power and the scanning speed. Under low energy input, the melting depth is relatively small. As shown in Fig.2 (a), when the melting depth is smaller than the layer thickness of the powder bed, the molten metal liquid will not be able to spread out and form good contact with the substrate. In addition, the existing time of the molten state is not long enough and the viscosity of the molten metal is not low enough. This allows only several neighboring melted powders to merge together and form a bigger ball to minimize the surface energy, resulting in the formation of isolated droplets. If the input energy goes higher, the melting depth is larger than the layer thickness of the powder bed, which means part of the substrate or the previously fabricated layers gets remelted, as shown in Fig.2 (b). The remelted part acts as a bridge of liquid connecting the melted powders. The good contact conditions promote the consolidation of the melted powders. The discontinuous droplets are then avoided and the continuous track is formed.

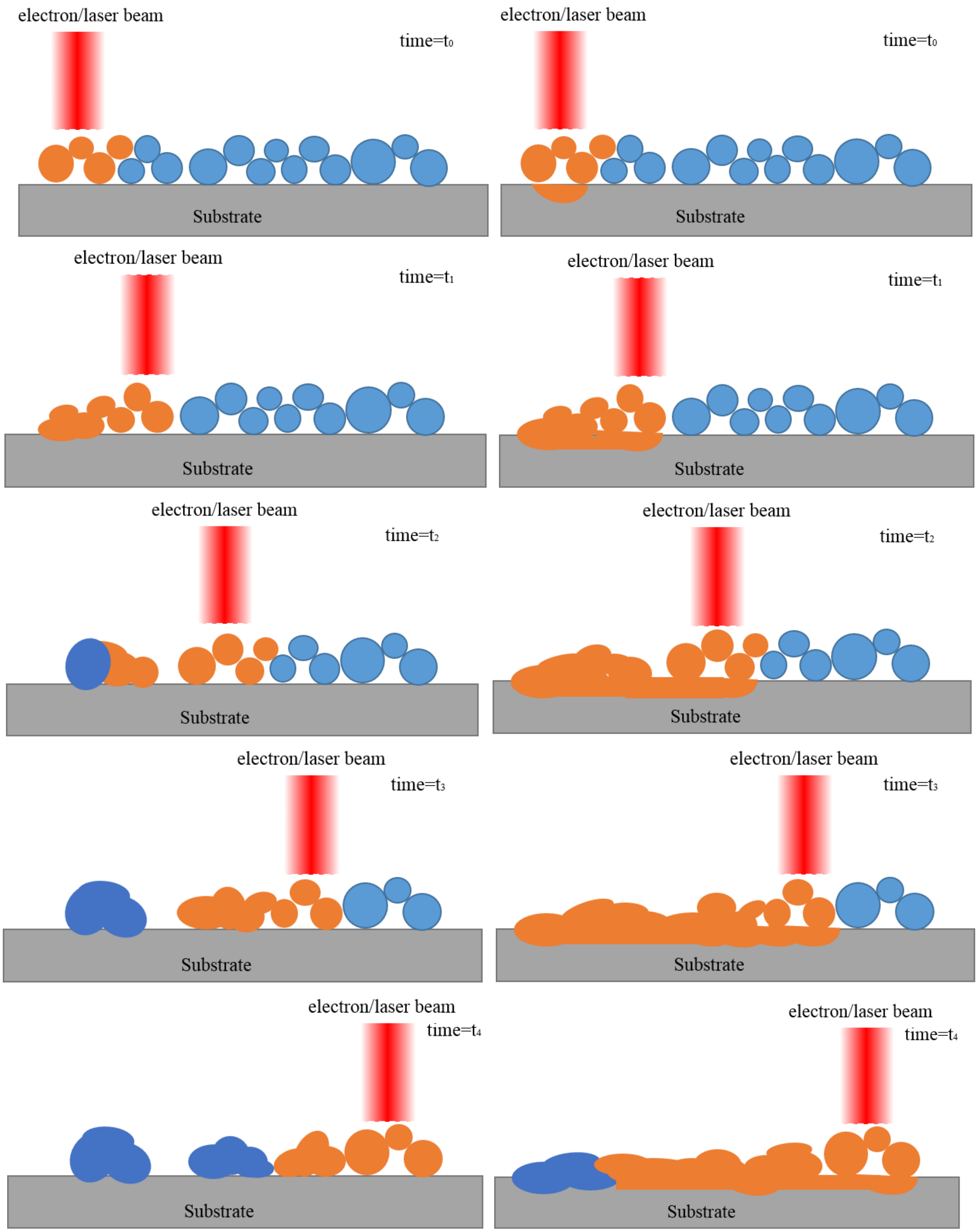

(a) formation of droplets (b) formation of a continuous track

Fig.2 Schematic diagram of the formation of droplets and a continuous track (side view)

The formation mechanism of the distortions is schematically illustrated in Fig.3. The blue circles represent unmelted powders, the orange portions represent the molten metal and the pink circle represents the electron beam which is moving up. The red dashed-dotted lines with *width-1* represent the melting boundaries. Only if the majority of one powder is located inside of the boundaries will the powder be melted. Because of the random arrangement of the powder bed, some powders outside but close to the boundaries stay unmelted and become in contact with the molten liquid inside but remain close to the boundaries. Then because of the surface tension force between the molten liquid and the unmelted powders, the molten liquid will be tightly attached to the unmelted powders, shown in the purple dashed boxes. The random attachments not only results in the distortions of the single track, but also lead to the fluctuations in the height of the solidified track.

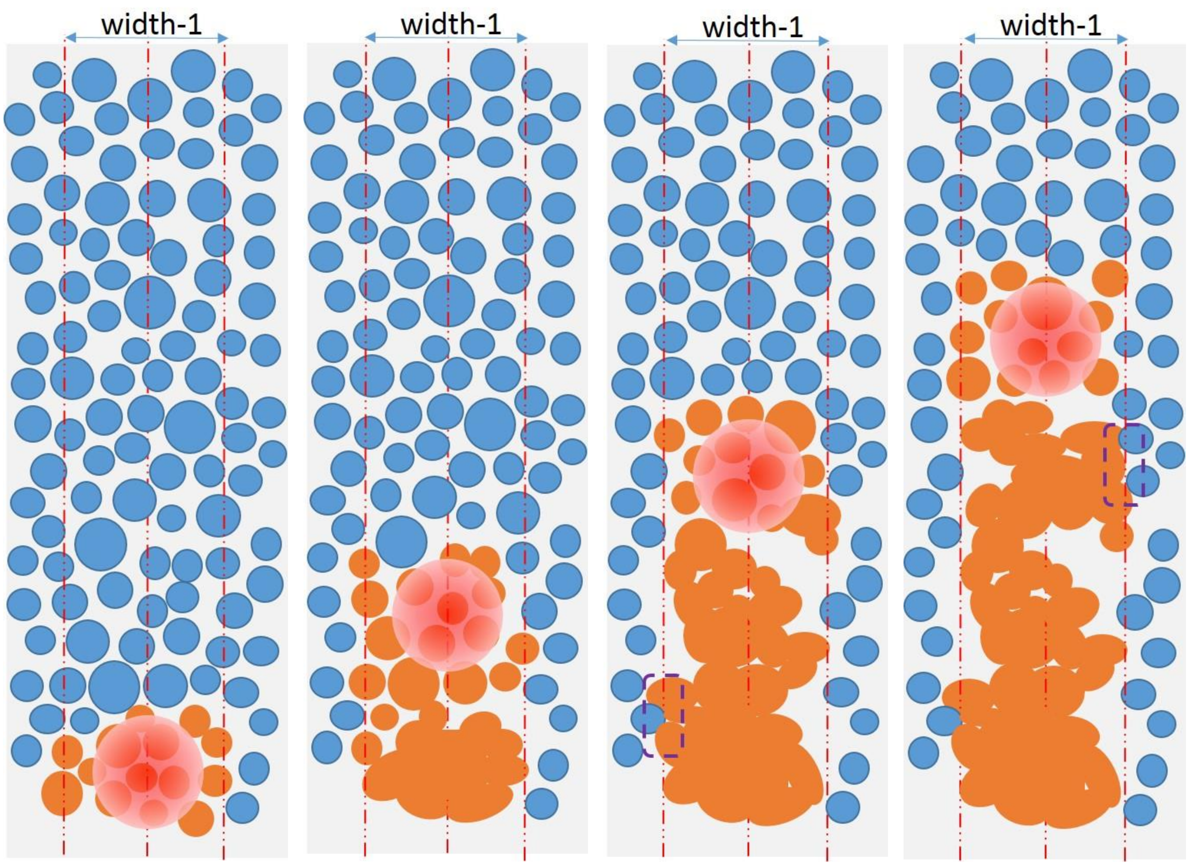

(a) t_1 (b) t_2 (c) t_3 (d) t_4

Fig.3 Schematic diagram of the formation of the distorted single track (top view)

In addition, since the powder bed is not dense, the volume of the solidified continuous track is smaller than the volume of the porous powder bed. This phenomenon is called powder bed shrinkage. In the ideal situation where none of the molten metal get attached to the unmelted powders outside the boundaries, the molten metal will shrink into a perfectly straight segmental cylinder with the remelted region of the substrate and the width of the solidified straight track will be the width of the remelted region of the substrate. We name the width of the remelted region of the substrate as *width-2*. In reality, it is hard to avoid the attachment between the molten metal and the unmelted powders and the resultant distortions. But the average width of the distorted track should be approximately close to the width of the remelted region of the substrate, *width-2*, due to the conservation of mass. Therefore, the distortion could be quantified as the difference between *width-1* and *width-2*.

The key assumption in the aforementioned physical models is that the surface tension force between the molten liquid and unmelt powders is the dominant driving force in the formation process of distorted single tracks. From the experimental image in Fig. 1(b), we can see the texture of the surface of the single track which illustrates the viscous flow. But the texture is also distorted to the boundaries, which proves that the surface tension force at the boundaries is dominant. The aforementioned processes could also be demonstrated by 3-D mesoscopic models tracing individual powders. However, the 3-D mesoscopic models are too complicated and computationally expensive for most researchers and engineers in the manufacturing area. Based on the aforementioned physical models, we found the remelting depth of the substrate (or the previously fabricated layers) was the key factor to determine the formation of the discontinuous droplets, and the difference between the melting width of the powder bed and the remelting width of the substrate determined the magnitude of the distortion. The key sizes related to the droplets and the distortions could be predicted using simplified heat transfer simulations. Here, we must emphasize that the numerical model is built based on the proposed physical model and the numerical model is not able to directly demonstrate the effectiveness of the physical model. In other words, the current numerical model is not able to provide the prediction of the realistic shapes of distorted single tracks and droplets, which is on-going work.

The challenges of the numerical model are mainly located on the accuracy of the predictions while considering the complexity caused by the powder bed. In this study, we proposed a new material model which changed the properties, especially the thermal conductivity, of the powder bed by tracing the state of the powder bed. Define a state variable F_s as the following equation, which represents the sintering status of the powder bed. T_p denotes the historically peak temperature of the powders during the sintering process, which is no higher than the liquidus temperature T_l and no lower than the solidus temperature T_s. Then F_s always falls between 0 and 1. It should be noted that the increase of F_s is inevitable.

$$F_s = \frac{T_p - T_s}{T_l - T_s}$$

The sintered powders have the thermal conductivity dependent on the state variable as defined as follows, where λ_b and λ_p are the thermal conductivity of the bulk material and the discrete powders, respectively. In this study, $\lambda_p \approx 0.02\lambda_b$.

$$\lambda = \lambda_b F_s + \lambda_p(1 - F_s)$$

The numerical heat transfer model was built using the Finite Element Method (FEM). The temperature T along with time t is governed by the following equations.

$$\lambda\nabla^2 T + q = \rho c \frac{\partial T}{\partial t} \quad \text{in the domain}$$
$$\lambda\nabla \mathrm{T} = \overline{q_s} \quad \text{at the boundaries}$$
$$T = \overline{T_s} \quad \text{at the boundaries}$$

In this study, q is the input body heat flux from the interactions between the electron beam and the material. The detailed description of the heat source model could be referred to [6]. $\overline{q_s}$ denotes the heat flux through the boundaries and only the radiation of the top surface was considered in this study. $\overline{T_s}$ is the fixed temperature of 900K at the bottom surface in this work.

$$q(x,y,z) = Q * \frac{3}{\pi R^2} \exp(-3 \cdot \frac{(x-x_s)^2 + (y-y_s)^2}{R^2}) * 114 \exp(- \frac{(z-0.004)^2}{0.005^2}) \quad x, y, z \text{ in mm}$$

$$q_R = -A \cdot \sigma \cdot \varepsilon (T^4 - T_a^4) \qquad \varepsilon = 0.2$$

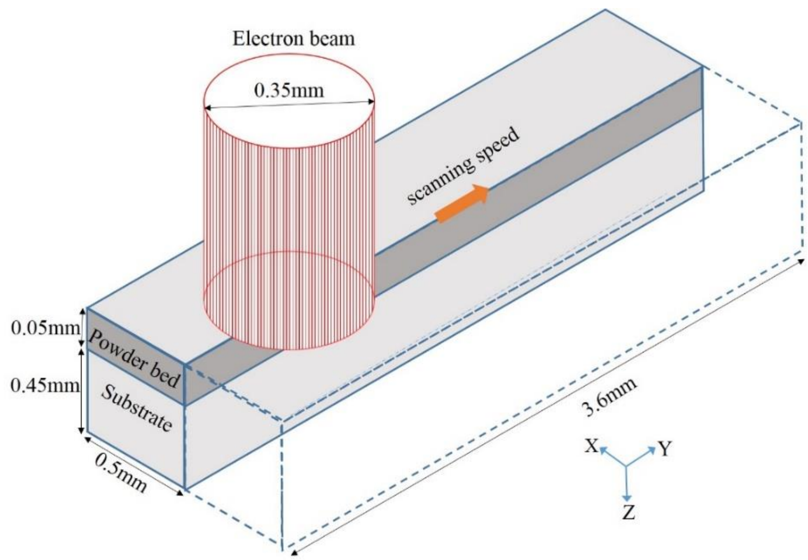

Fig.4 Heat transfer model

Experiment

The experiments were conducted using the Arcam S400 system. The material of the powder and the substrate is Ti-6V-4V. The material properties [7] are listed in Table.1. The temperature-dependence was ignored for simplicity in the numerical model.

Table.1 Properties of Ti-6Al-4V

Density (kg/m^3)	**Specific heat (J/kg)**	**Thermal conductivity (W/m·K)**	**Latent heat (J/kg)**
4400	700	15	286000

Generally, the Electron Beam Melting consists of four steps [8].

(1) Spread powders on the base plate. The substrate used in this study was 170mm*170mm*10mm.

(2) Preheat the powder bed using a defocused electron beam to prevent powder scattering. The temperature of the bottom face was fixed at 900K, monitored by the thermocouple attached at the bottom face.

(3) Melt the powder using focused electron beam.

(4) Move down the platform by one layer thickness which, in this study, was fixed at 0.05mm.

Results and discussion

In this conference, we just showed the preliminary results. We will publish a formal journal article after more results are obtained. When the scanning speed was 0.05m/s and the electron beam current was 0.5mA, discontinuous droplets were formed. The experimental and simulated results are shown in Fig.5. The simulated melting depth was 50μm, which means the simulated remelting depth was 0. According to the aforementioned physical model, the lack of the remelting of the substrate leads to the formation of the droplets. The droplets were validated by the experimental results. The simulated *width-1* was 360μm while the measured *width-1* was 334μm, which also shows the good agreement. Therefore, the proposed physical mechanism and the numerical model of the formation of the droplets are demonstrated to be able to predict the formation of the droplets.

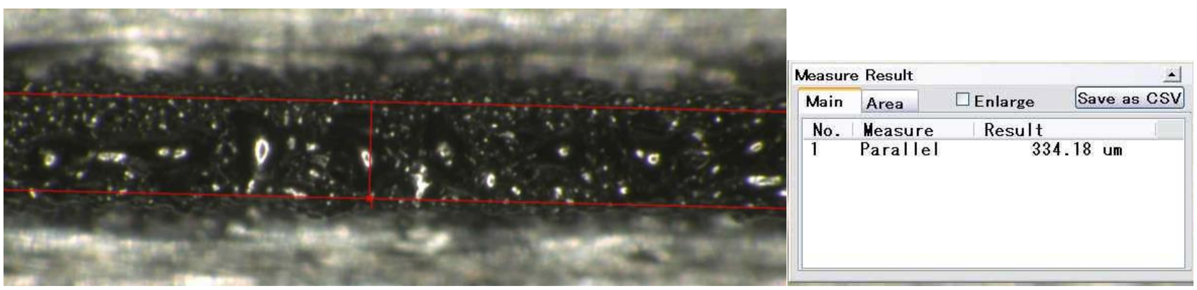

(a) experimental image and measurement

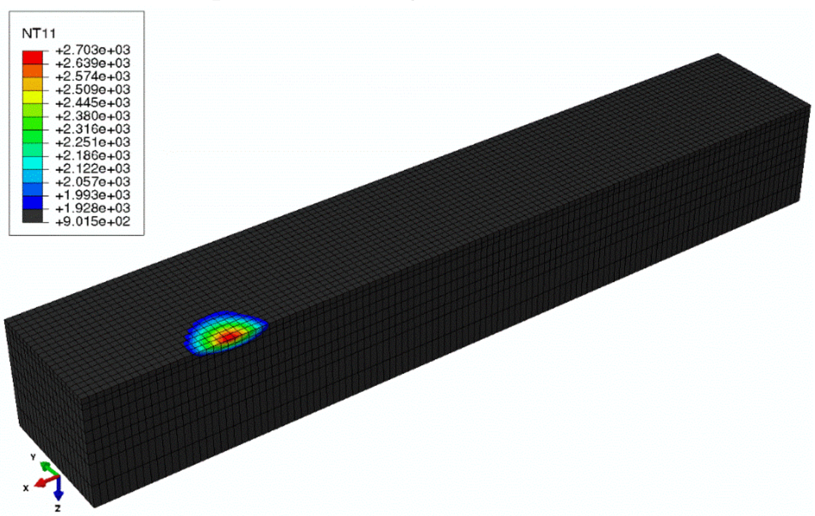

(b) thermal simulation result

Fig.5 Experimental and simulated results for the specimen fabricated with 0.5mA, 0.05m/s

When the scanning speed was fixed at 0.05m/s and the electron beam current was increased to 1mA and 1.5mA, continuous distorted tracks were formed. The experimental results are shown in Fig.6, and the simulated and experimental data of *width-1* and *width-2* are listed in Table.2. The simulation results are in good agreements with the experiments, which proves the ability of the physical and numerical models to quantitatively predict the distortions of the single track formation. The errors are from the simplifications of the models, which pay the price of the simplicity of the models.

In some sense, the distortion is unavoidable for the powder bed fashioned additive manufacturing technologies because of the unavoidable random attachment between melted metal and unmelted powders near the boundaries. But it is possible to reduce the magnitude of the distortion by minimizing the difference between *width-1* and *width-2*. One approach is to reduce the porosity of the powder bed, e.g. employing the optimal size distribution and improving machine structure of the powder bed spreader. A denser powder bed results in smaller shrinkage and distortion. Another approach is to change the scanning strategy and the fabrication parameters. In this study, the beam current was the only parameter varied, for it has the strongest effect. Additional parameters, such as scanning speed, layer thickness and preheating temperature, are also effective to control the distortions.

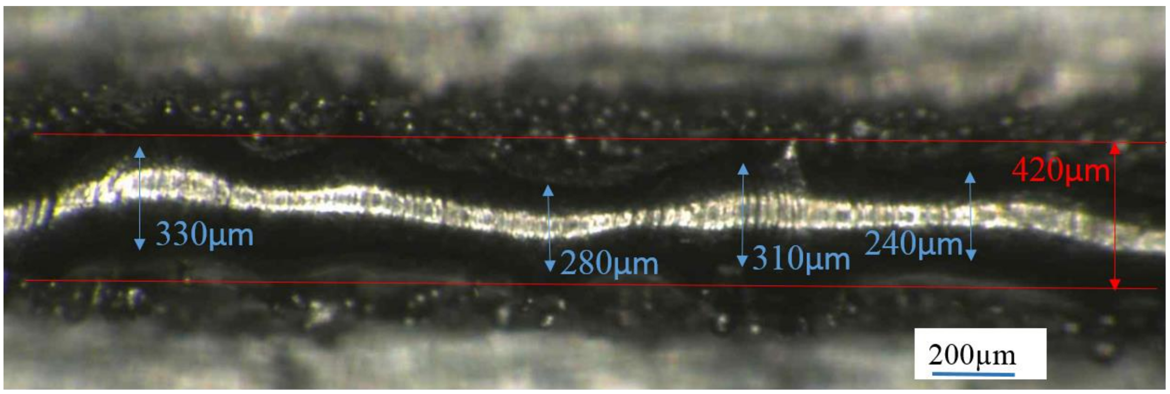

(a) 0.05m/s, 1mA

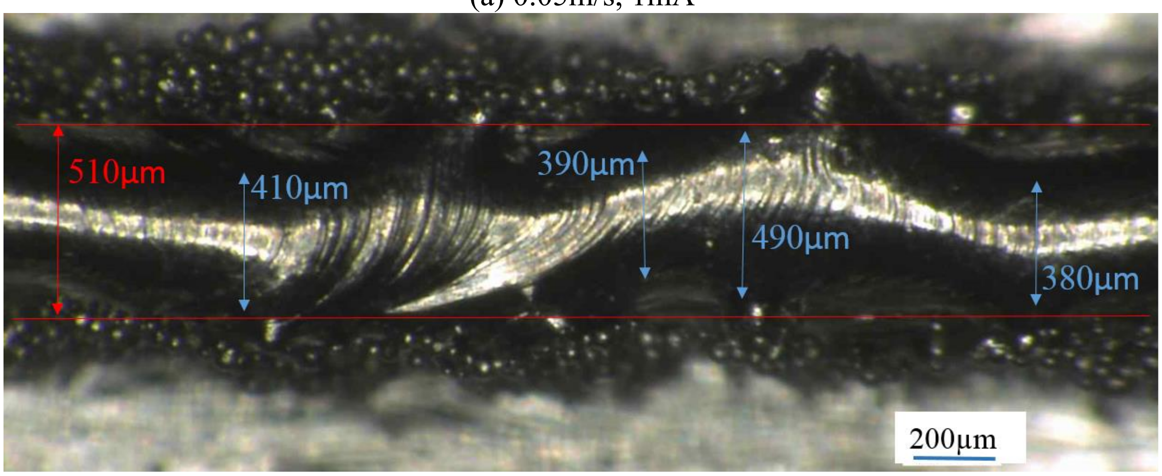

(b) 0.05m/s, 1.5mA

Fig.6 Experimental images and measured results

Table.2 Simulated and experimental results

		***width-1* (mm)**	***width-2* (mm)**
0.05m/s, 1mA	simulation	450	310
	experiment	420	290
0.05m/s, 1.5mA	simulation	490	420
	experiment	510	420

Conclusion

In order to achieve high-quality products by Selective Beam Melting technologies, discontinuous droplets and distortions of the continuous tracks were investigated. The physical mechanisms of the formations of the droplets and distortions were proposed and the heat transfer simulations using FEM were established to predict the possibility of forming droplets and the magnitude of the distortion. The experiments using EBM were then conducted to validate the physical and numerical models. The good agreements of the simulated and experimental results demonstrated that the proposed models are simple and efficient to provide quantitative predictions. The numerical model was realized in commercial FEM software, so it can be easily employed by researchers and engineers in manufacturing area.

Acknowledgements

The first author is currently a visiting Ph.D. student at the Department of Mechanical Engineering, Northwestern University, and he would like to thank China Scholarship Council (CSC) for the financial support. This research work was performed under the financial assistance award 70NANB13Hl94 from National Institute of Standards and Technology, and 70NANB14H012 from U.S. Department of Commerce, National Institute of Standards and Technology as part of the Center for Hierarchical Materials Design (CHiMaD).

References

1. Childs, THC and Hauser, C and Badrossamay, M, Mapping and modelling single scan track formation in direct metal selective laser melting, CIRP Annals-Manufacturing Technology, 53, 191-194 (2004)

2. Yadroitsev, I., Gusarov, A., Yadroitsava, I., and Smurov, I., Single track formation in selective laser melting of metal powders, Journal of Materials Processing Technology, 210(12), 1624-1631 (2010)

3. Zäh, M. F. and S. Lutzmann, Modelling and simulation of electron beam melting, Production Engineering, 4(1), 15-23 (2010)

4. Dai, D. and D. Gu, Tailoring surface quality through mass and momentum transfer modeling using a volume of fluid method in selective laser melting of TiC/AlSi10Mg powder, International Journal of Machine Tools and Manufacture, 88(0), 95-107 (2015)

5. Korner, Carolin, Elham Attar, and Peter Heinl, Mesoscopic simulation of selective beam melting processes, Journal of Materials Processing Technology, 211(6), 978-987 (2011)

6. Yan, W., Smith J., Ge, W., Lin, F., and Liu, W., Multiscale modeling of electron beam and substrate interaction: a new heat source model, Computational Mechanics, 1-12 (2015)

7. Jamshidinia M., Kong F., Kovacevic R., Numerical modeling of heat distribution in the electron beam melting® of Ti–6Al–4V. Journal of Manufacturing Science and Engineering, 135(6):061010 (2013)

8. Ge W., Guo C., Lin F., Effect of process parameters on microstructure of TiAl alloy produced by electron beam selective melting. Procedia Engineering 81:1192–1197 (2014)